Proceedings of the 16th European VLBI Network Symposium
Ros, E., Benke, P., Dzib, S., Rottmann, I., & Zensus, J.A. (eds.)
September 2nd-6th 2024, Bonn, Germany

Breaking news from high-mass star formation: recent VLBI contributions

G. Surcis

INAF - Osservatorio Astronomico di Cagliari, Via della Scienza 5, I-09047, Selargius, Italy

Abstract. The formation process of high-mass stars ($M > 8$ M$_\odot$) is still unclear; this is mainly due to their fast evolution and large distances that make it very difficulty to observe them in detail. However, many observational and theoretical efforts have been made in the last decades that have shed light on some aspects of the formation process. For instance, it has been shown that molecular outflows are essential during the formation process as much as the accretion disks, similarly to what happens during the formation of low-mass stars. Furthermore the magnetic field is considered playing an important role in the formation of massive young stellar objects (YSOs), for instance in launching and shaping molecular outflows. Three of the most recent results in the field, which were obtained through the VLBI technique, are highlighted in this proceeding. In particular, among these, the results obtained with the EVN toward the high-mass star-forming region W75N(B) will be presented more extensively, including a comparison with the most recent ALMA results.

1. Introduction

Stars in the Universe are divided into two main classes according to their mass: low-mass stars ($M < 8$ M$_\odot$) and high-mass stars ($M > 8$ M$_\odot$). Although, sometimes, stars with a mass around 8 M$_\odot$ are classified as intermediate-mass stars. While the formation process of low-mass stars has been quite well established, the formation process of high-mass stars is still debated. An evolutionary scenario of high-mass star formation (HMSF) based on observational inputs has been outlined by several authors (e.g., Motte et al. 2018; Urquhart 2024) and a brief summary of it is reported here. High-mass stars form in the densest parts of giant molecular clouds that are called clumps (size $\sim$1 pc, M = 500$-$1000M$_\odot$). These are gravitationally bound and pass from a quiescent state (starless massive dense core phase) to a global controlled collapse by accreting material from their surroundings through filaments, ultimately forming low-mass prestellar cores that become protostar in about 10^4 year (protostellar massive dense core phase). After $\sim 10^5$ years more, the high-mass protostellar phase starts, even though they still harbor low-mass stellar embryos. At this stage the accretion disks are already formed and, if their accretion rates are efficient, the high-mass protostars also drive bipolar outflows. Now the masers arise (mainly OH, H_2O, and CH_3OH) around disks and outflows. When the stellar embryos reach more than 8 M$_\odot$ the high-mass protostars develop first hypercompact and then ultra-compact H II regions, which are quenched by infalling gas or confined to the photoevaporating disks. Finally, the ultraviolet radiation from the stellar embryos produces the H II region and the gas accretion toward the newborn star slows to a halt, this phase is called H II region phase and lasts about $10^5 - 10^6$ years. The high-mass star is formed.

The protostellar phase of high-mass stars is very difficult to observe and study; mainly because the massive protostars are rare, evolve quickly, and they are located far from us. In addition, they form exclusively in clusters where they are deeply embedded, making the observations of individual protostars very difficult if not impossible. However, the formation scenario described above has been drawn thanks to the advent of new instruments in the last decades that have also helped to guide more sophisticated simulations. In the past, radio interferometry technique, even as Very Long Baseline Interferometry (VLBI), was fundamental to observe some of the aspects of high-mass star-formation, such as the large-scale molecular outflows and the H II regions, and to measure the proper motion and the polarized properties of masers, which provide information about the gas motion and the magnetic field along outflows and around possible disk structures. However, only with the upgrade of existing instruments (e.g., the Karl G. Jansky Very Large Array, VLA) and the new generation of instruments (e.g., the Atacama Large Millimeter/submillimeter Array, ALMA) some features have been directly imaged, among them: the accretion disks (e.g., Sanna et al. 2021) with their magnetic field (e.g., Girart et al. 2018), the interplay between the large-scale outflows and the small-scale jets (e.g., Goddi et al. 2020), and the hourglass shape of magnetic field that is typical of low-mass protostars (e.g., Saha et al. 2024). Nevertheless, even though ALMA is playing a major role nowadays, VLBI is still able to provide at millarcseconds (mas) resolution important insights to the investigation of the HMSF. In this contribution, I will present some highlights of three of the most recent and important results obtained with the VLBI toward three massive young stellar objects (YSOs): G358.93-0.03-MM1 (Burns et al. 2023), IRAS 21078+5211 (Moscadelli et al. 2022, 2023, 2024), and W75N(B) (Surcis et al. 2023, Gómez et al. 2023).

2. High-mass star formation: VLBI highlights

2.1. G358.93-0.03-MM1

G358.93-0.03-MM1 is a massive YSO (M $\sim$ 11 $M_\odot$; Stecklum et al. 2021) located at a distance of $6.75^{+0.37}_{-0.68}$ kpc (Reid et al. 2014). This YSO was little studied till 2019 when it went through an accretion burst identified thanks to a 6.7 GHz CH_3OH maser flare, which passed from a peak flux of $\sim$10 Jy to $\sim$100 Jy in a few weeks (Sugiyama et al. 2019) and reached a maximum flux of $\sim$900 Jy in a couple of months (e.g., Burns et al. 2020). The YSO was then heavily observed at various frequencies, not only radio, and with different facilities all over the world by the Maser Monitoring Organization[1] (M2O; Burns 2024). In particular, Burns et al. (2020) monitored the 6.7 GHz CH_3OH masers with several VLBI facilities, among which the European VLBI netwrok (EVN), from February to September 2019. The masers showed a rapid transformation of their circular distributions only few weeks apart, passing from a 40 mas radius to a 77 mas radius in only 26 days, indicating the possible presence of an expanding ring of gas at sub-luminal velocity ($> 4\%$ of c). However, this velocity is extremely higher than the typical CH_3OH maser proper motions (≤ 10 km s^{-1}), suggesting that the fast morphological transformation could not be attributed to physical motions of the gas in the inclined accretion disk ($i = 21° \pm 5°$). The 6.7 GHz CH_3OH maser transition is pumped by infrared photons emitted by the protostar at the center of the YSO, therefore the fast transformation of the maser distributions can be explained by the outward propagation of the favorable maser conditions, the so-called "heatwave", and the sequential arising and quenching of masers at every-increasing radii (Burns et al. 2020).

More recently, Burns et al. (2023) noted that the six VLBI epochs effectively sample six radially incremented static snapshots of the spatio-kinematics of gas in the region around the protostar. Therefore, a more accurate analysis of the maser distributions over the six VLBI epochs requires combining all of these concentric snapshots in a single mas-scale map ("heatwave mapping"), which leads to a discretely sampled map of the kinematic structure as traced by maser-emitting gas around the YSO (see Fig. 1). From this map they were able to determine that the maser spots are mainly located along four different spiral structures. From the analysis of the position-velocity profile of the combined data set the gas also shows Keplerian rotation. Therefore, the 6.7 GHz revealed the presence in G358.93-0.03-MM1 of a Keplerian accretion disk with a four-arm spiral structure. Burns et al. (2023) have then shown that "heatwave mapping" of 6.7 GHz CH_3OH masers can be used to resolve the spatio-kinematics of accretion disks at the angular resolution necessary to characterize disk substructures in high-mass protostars.

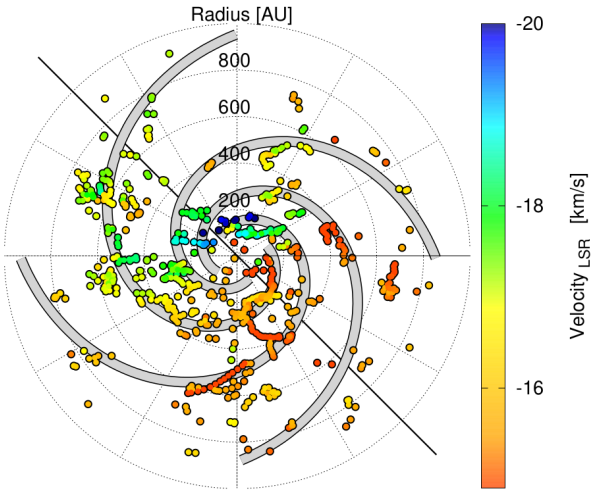

Fig. 1. Figure reproduced from Burns et al. (2023). Spotmap of the combined six VLBI epochs centered on the position of the massive YSO G358.93-0.03-MM1. The colored circles represent the 6.7 GHz CH_3OH maser spots with the spiral arms (thick grey lines) as identified by Burns et al. (2023).

2.2. IRAS 21078+5211

IRAS 21078+5211 is a star-forming region at a distance of 1.63 $\pm$ 0.05 kpc (Xu et al. 2013) that harbours a cluster of YSOs. The most massive YSO of the region (5.6 $\pm$ 2 $M_\odot$; Moscadelli et al. 2021) shows a disk-jet system, that was imaged with the NOrthern Extended Millimeter Array (NOEMA; Moscadelli et al. 2021) and the VLA (Moscadelli et al. 2016), and host a cluster of 22 GHz H_2O masers whose proper motions are collimated northeast-southwest along the major axis of the thermal radio jet (PA=49°; Moscadelli et al. 2016).

In October 2020, Moscadelli et al. (2022) observed the H_2O masers with sensitive Global VLBI observations and, besides detecting many more masers, they noted a significant change of their spatial distribution. In particular, the masers revealed spiraling streamlines launched from the disk. These observations were also performed in full polarization mode allowing the detection of the linearly and circularly polarized emission in a handful of maser features (Moscadelli et al. 2023). From these the morphology and strength of the magnetic field was estimated, and its vectors were found to be consistent with resistive-radiative-gravito-magnetohydrodynamic simulations of a disk wind performed by the same authors, where the streamlines are found to be flowing outwards along a helical magnetic field (Moscadelli et al. 2023).

Recently, between March and October 2023, Moscadelli et al. (2024) performed new multi-epoch Very Long Baseline Array (VLBA) observations of the 22 GHz H_2O masers with the aim to measure their

[1] M2O is a community of multiwavelength observers, astrophysicists and maser theoreticians pursuing research into time-variable astrophysical phenomena traced by maser emission, see https://www.masermonitoring.com for more details.

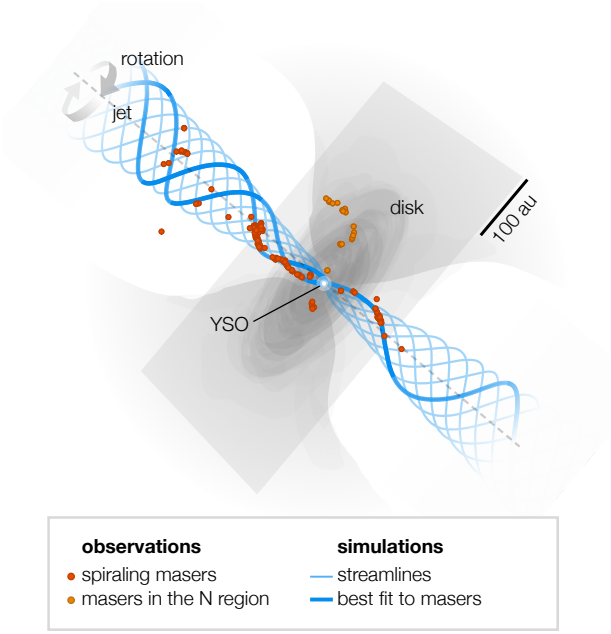

Fig. 2. Figure reproduced from Moscadelli et al. (2024). Three-dimensional view of the magnetohydrodynamic disk wind in IRAS 21078+5211.

3D velocities in the disk wind streamlines. They found that the morphology of the maser distribution varied a bit in three years, but more importantly they found that the velocities vectors of the masers are generally consistent with the spiraling motion of the gas but not in the North region (N region). Here, the masers move at small speed along a direction parallel to the disk, suggesting that these masers trace a radially expanding shock front due to a magnetic pressure that dominates at radii larger than 50 au. Thanks to all the results obtained since 2020, Moscadelli et al. (2024) were able to prove, by comparing with their final simulations (Fig. 2), that the H_2O masers VLBI observations can determine the launching mechanism of protostellar winds and in particular that magnetohydrodynamic disk wind could be the common launching mechanism of protostellar winds also from high-mass protostars.

2.3. W75N(B)

The H_2O masers in VLA 2 are not tracing a symmetric expansion as it was reported previously (Surcis et al. 2023). Actually, in the past the comparison between different epochs was done by assuming that the center of the maser distributions was always the same (e.g., Surcis et al. 2014), this because not every of those observations were performed in phase-referencing mode as it was instead the case in the new four epochs, when to measure the absolute positions of the H_2O masers was possible. The expansion of the gas, which is determined from the proper motions of the masers (see Fig. 4), is faster toward southwest (78 km s^{-1}) and southeast (38 km s^{-1}); in the northwest is around 26-28 km s^{-1}; while in the northeast the expansion of the gas is prevented by the possible presence of a very dense gas (Surcis et al. 2023). Recently, Gómez et al. (2023) observed H_2CO and SiO emissions toward W75N(B) with ALMA. These two emissions are good tracers of dense gas and shocked gas, respectively. They confirmed the presence of a very dense H_2CO clump ($n_{H_2} < 3 \times 10^8$ cm^{-3}) to the north-northeast of VLA 2 that halts the expansion of the H_2O masers toward northeast (see Fig. 4). In addition, Gómez et al. (2023) identified a SiO toroid surrounding VLA 2, the one suggested by Carrasco-González et al. (2015), and a wide-angle SiO outflow originating from the outer regions of the toroid. The magnetic field vectors around VLA 2 is found, as expected, to be generally perpendicular to the proper motions of the H_2O masers, but in the northeast, it becomes parallel after encountering the H_2CO dense clump (see Fig. 3). Indeed, if the magnetic field is decomposed in two components, one perpendicular to the shock propagation direction (coincident with the direction of the masers proper motions) and the other one parallel to it, we have that the perpendicular component is compressed by the passage of the shock and dominate the parallel one, which remains unaffected. Consequently, the resulting magnetic field probed by the H_2O masers is expected to be along the shock front. This is not the case in the northeast after the shock encounters the very dense clump. Here, the compression of the gas due to the passage of the shock is inefficient and the perpendicular component of the magnetic field does not longer dominates over the parallel one, which is originally stronger. If the magnetic field in the northeast region of VLA 2 is compared with the large-scale magnetic field reported by Palau et al. (2021), it is found to be morphologically consistent with it. W75N(B) is a high-mass star forming region at a distance of 1.30±0.07 kpc (Rygl et al. 2012) in the Cygnus X complex. Several massive YSOs have been identified in the region, among them VLA 1, VLA 2, and VLA 3 are thought to be in three evolutionary stages. VLA 1, which is thought to be the most evolved, is at the early stage of photoionization and it is driving a thermal radio jet oriented northeast-southwest with a position angle of about 40° (e.g., Rodríguez-Kamenetzky et al. 2020). Also VLA 3 is driving a thermal radio jet oriented northwest-southeast (Rodríguez-Kamenetzky et al. 2020). The youngest source is VLA 2, located about 1000 au southeast from VLA 1, and its radio morphology was observed varying in few decade (e.g., Carrasco-González et al. 2015). Indeed, in 1996 its radio continuum emission had a compact ($\leq$ 160 au) roundish morphology (Torrelles et al. 1997) that became elongated in the northeast-southwest direction (220$\times$ $\leq$ 160 au, PA=65°) in 2014 (Carrasco-González et al. 2015). Carrasco-González et al. (2015) determined that VLA 2 is a thermal, collimated ionized wind that must be surrounded by a dusty disk (PA $\approx -25°$) responsible for the morphology variation. This variation was also observed in the 22 GHz H_2O maser distribution that

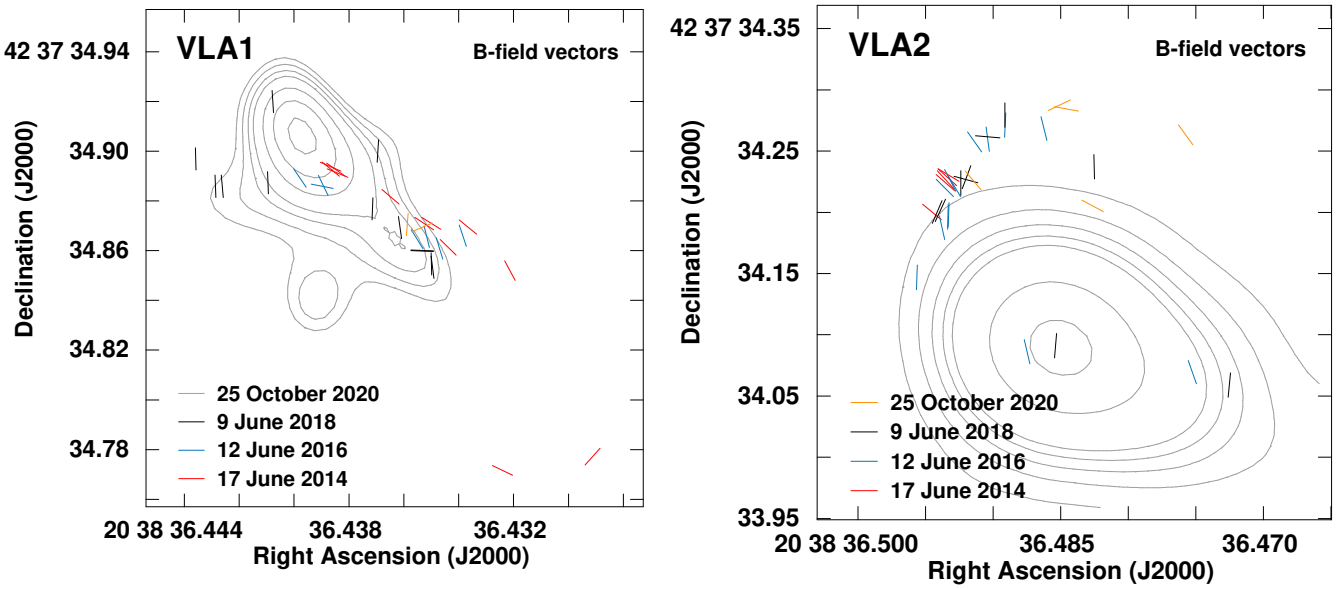

Fig. 3. Magnetic field vectors on the plane of the sky as estimated from the linearly polarized H_2O masers detected along W75N(B)-VLA 1 (left panel) and around -VLA 2 (right panel) during the four EVN epochs by Surcis et al. (2023) and superimposed to their continuum maps at Q-band (Rodríguez-Kamenetzky et al. 2020) and K-band (Carrasco-González et al. 2015), respectively. For more details see Surcis et al. (2023).

were monitored with the VLBI from 1996 to 2012. In particular, the maser distribution was quasi-circular from 1996 to 2005 (Torrelles et al. 2003, Surcis et al. 2011), showing a symetrical expansion, and becoming elliptical since 2007 (Kim et al. 2013, Surcis et al. 2014), following the exact morphology change observed in the continuum emission. Therefore the H_2O masers might be tracing the evolution from a non-collimated to a collimated outflow. In the same timescale, the H_2O maser detected toward VLA 1 showed a persistent linear distribution (PA $\approx 43°$) along the thermal radio jet (e.g.; Surcis et al. 2014). Only one H_2O maser was associated with VLA 3 and only in 1996 epoch (Torrelles et al. 1997). Two of the H_2O maser observations (in 2005 and 2012) were perdormed in full polarization mode allowing the study of the magnetic field around VLA 1 and VLA 2. Surcis et al. (2014) showed that the magnetic field around VLA 1 was always oriented along the direction of the thermal radio jet, while the orientation of the magnetic field around VLA 2 changed consistently with the major-axis of the masers distribution.

The peculiarity of the H_2O maser expansion with the contemporary variation of the magnetic field around VLA 2, together with the presence of the nearby VLA 1 source, make W75N(B) one of the most interesting high-mass star-forming region for investigating the evolution of early massive YSOs. For this reason, a VLBI monitoring project of 22 GHz H_2O maser emission in full polarization and phase-referencing mode was performed with the EVN by Surcis et al. (2023). They observed every two years from 2014 to 2020 for a total of four epochs.

Surcis et al. (2023) found that the H_2O masers around VLA 1 are constantly distributed along the major axis of the thermal radio jet during the four epochs and they probe a nondissociative shock produced by the expansion of the thermal jet. From the linearly polarized maser emission it is possible to estimate the orientation of the magnetic field vectors and by comparing those estimated in similar location, but in different epochs, it is clear that they all seem to represent a quasi-static magnetic field (see Fig. 3). Therefore, the magnetic field vectors estimated from the H_2O masers in one epoch are representative of the magnetic field in their locations rather than in that time. Consequently, the magnetic field vectors of all the EVN epochs can be gathered together and considered as measurements carried out at the same time. In the case of VLA 1 this shows that the magnetic field is along the thermal jet and it bends toward the south at the southwest end of the thermal jet and toward the north at the northeastern end.

3. Conclusions

Despite the great contribution provided by ALMA and the upgraded instruments like NOEMA and the VLA, the three highlights that I have summarized in this conference proceeding show that classical VLBI observations can still play a crucial role in the modern investigation of HMSF. In particular, if their results are analyzed in synergy with results obtained with other instruments (G358.93-0.03-MM1 and W75N(B)) or with simulations (IRAS 21078+5211).

The future of the VLBI in this research field points towards simultaneous multi-frequencies observations. For instance studying simultaneously more maser emissions, from the same or different maser species, will help to de-

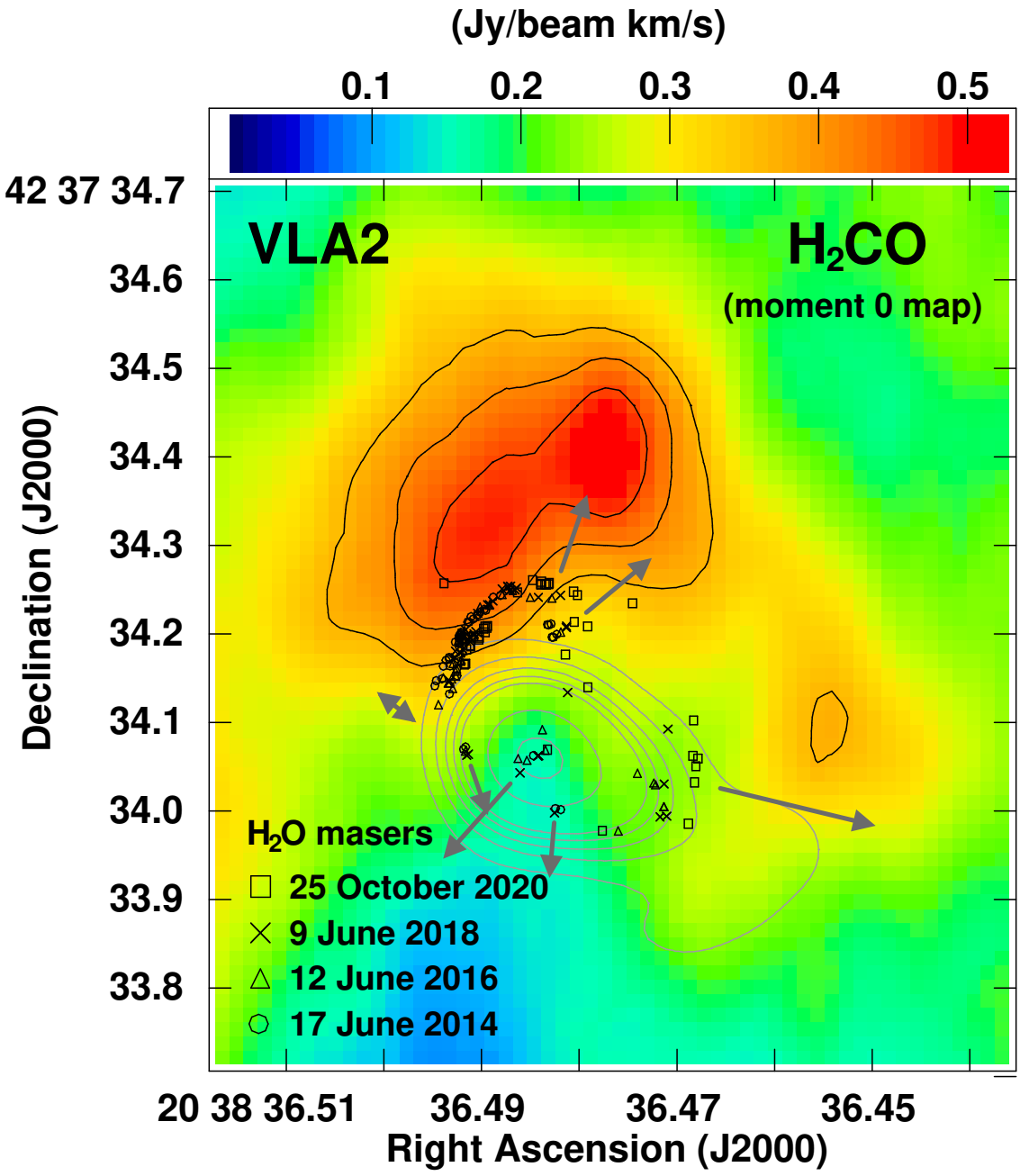

Fig. 4. Comparison of the H_2O masers detected toward W75N(B)-VLA 2 in the four EVN epochs (2014.46, 2016.45, 2018.44, and 2020.82) by Surcis et al. (2023) and superimposed to the continuum map at K-band of the thermal, collimated ionized wind emitted by VLA 2 (gray contours; Carrasco-González et al. 2015) and to the integrated intensity image (moment of order 0) of the H_2CO [3(0,3)-2(0,2)] emission line observed with ALMA (black contours; Gómez et al. 2023). The positions of the masers and of the K-band continuum are corrected assuming the proper motion of the subregion W75N(B) equal to the median proper motion measured for the 6.7 GHz CH_3OH maser features by Rygl et al. (2012), $\langle\mu_\alpha\rangle = (-1.97 \pm 0.10)$ mas yr^{-1} and $\langle\mu_\delta\rangle = (-4.16 \pm 0.15)$ mas yr^{-1}. The arrows represent the direction of the H_2O maser proper motions on the plane of the sky as reported by Surcis et al. (2023). For further image details see Surcis et al. (2023) and Gómez et al. (2023).

termine some physical characteristics of the gas around massive YSOs that cannot be done with other observations yet. This kind of observations could be done relatively soon in Italy thanks to the recent equipment of the Korean compact three-band receiver (K-, Q-, and W-band) at the three Italian antennas (the so-called VLBI Italian Array, VITA). This kind of upgrade, with similar receivers, is also planned in several other antennas in Europe that will make the EVN the first continental VLBI network equipped with multi-frequency receivers.

Acknowledgements. I would like to acknowledge all my colleagues and collaborators who made it possible to achieve the results highlighted in this conference contribution.

References

Burns, R.A., Sugiyama, K., Hirota, T., et al. 2020, NatAs, 4, 506B
Burns, R.A., Uno, Y., Sakai, N., et al. 2023, NatAs, 7, 557B
Burns, R.A. 2024, IAU Symp., 380, 443
Carrasco-González, C., Torrelles, J.M., Cantó, J., et al., 2015, Science, 348, 114
Girart, J.M., Fernández-López, M., Li, Z.-Y., et al. 2018, ApJ, 856, 27G
Goddi, C., Ginsburg, A., Maud, L.T., et al. 2020, ApJ, 905, 25G
Gómez, J.F., Torrelles, J.M., Girart, J.M., et al., 2023, ApJL, 956, L45
Kim, J.-S., Kim, S.-W., Kurayama, T., et al. 2013, ApJ, 767, 86
Moscadelli, L., Sánchez-Monge, Á., Goddi, C., et al. 2016, A&A, 585, A71
Moscadelli, L., Beuther, H., Ahmadi, A. et al. 2021, A&A, 647, A114
Moscadelli, L., Sanna, A., Beuther, H., et al. 2022, NatAs, 6, 1068M
Moscadelli, L., Oliva, A., Surcis, G., et al. 2023, A&A, 680A, 107M
Moscadelli, L., Oliva, A., Sanna, A., et al. 2024, A&A, 690A, 81M
Motte, F., Bontemps, S., and Louvert, F. 2018 ARA&A, 56, 41
Palau, A., Zhang, Q., Girart, J.M., et al. 2021, ApJ, 912, 159
Reid, M., Menten, K.M., Brunthaler, A., et al. 2014, ApJ, 783, 130
Rodríguez-Kamenetzky, A.R., Carrasco-González, C., Torrelles, J.M., et al. 2020, MNRAS, 496, 3128
Rygl, K. L. J., Brunthaler, A., Sanna, A., et al. 2012, A&A, 539, A79
Saha, P., Sanhueaza, P., Padovani, M., et al. 2024, ApJ, 972L, 6S
Sanna, A., Giannetti, A., Bonfald, M., et al. 2021, A&A, 655A, 72S
Stecklum, B., Wolf, V., Linz, H., et al. 2021, A&A, 646A, 161S
Sugiyama, K., Saito, Y., Yonekura, Y., et al. 2019, ATel, 12, 446, 1
Surcis, G., Vlemmings, W.H.T., Curiel, S., et al. 2011, A&A, 527, A48
Surcis, G., Vlemmings, W.H.T., van Langevelde, H.J., et al. 2014, A&A, 565, L8
Surcis, G., Vlemmings, W.H.T., Goddi, C. , et al. 2023, A&A, 673, A10
Torrelles, J.M., Gómez, J.F., Rodríguez, L.F., et al. 1997, ApJ, 489, 744
Torrelles, J.M., Patel, N.A., Anglada, G., et al. 2003, ApJ, 598, L115
Xu,Y., Li, J.J., Reid, M.J., et al. 2013, ApJ, 769, 15X
Urquhart, J.S. 2024, IAU Symp., 380, 135U